Investigation of Mode and Modulation Responses in Semiconductor PS-DFB Lasers: Use of a Vector-Newton Method

Zhang Yejin[1], Zhu Lin[1], Gao Zhiguo[1], Chen Minghua[1], Dong Yi[1], Chen Weiyou[2], Liu Shiyong[2] and Xie Shizhong[1]

([1] *Department of Electronics Engineering, Tsinghua University, Beijing 100084, China*)
([2] *Department of Electronics Engineering, Jilin University, Changchun 130023, China*)

Abstract: A numerical model for steady state analysis and analytical expressions for the AM and FM modulation responses of DFB lasers are presented. The small signal modulation responses of 3 phase shift (PS) DFB is investigated for the first time. A new method (Vector-Newton method) to obtain multiple-longitudinal-mode of DFB lasers is used. It is demonstrated that this method is suitable for obtaining multiple-solution of high nonlinear equations. Longitudinal photon density distribution and multiple-longitudinal-mode of 3PS-DFB and simple-DFB lasers are analyzed. The results show that modulation response characteristics of 3PS-DFB laser is as good as that of DFB, and PS can weaken the longitudinal spatial hole-burning (LHSB) effect and is in favor of single longitudinal mode operating of lasers.

Key words: phase shift; DFB; vector; single mode; LHSB; modulation response
PACC: 4255P; 4260; 7340L; 7280
CLC number: TN248.4 **Document code**: A **Article ID**: 0253-4177(2002)09-0935-06

1 Introduction

Distributed feedback (DFB) semiconductor lasers are key devices for high-speed, long-haul communication links and broad-band information networks. As the fabrication technologies for producing these laser diodes become mature, modeling and simulation begin to play more important roles in the computer-aided engineering (CAE) of such devices for different applications. Most DFB laser models are basically one-dimensional, in the sense that they account for distributions of the optical field, the carrier, and the temperature along the laser[1~3]. Some 2-D or 3-D models for DFB lasers that consider both the transverse and the longitudinal effects have been reported[4~6]. In these models, transfer matrix method (TMM) is used to obtain a complex equation for the steady-state photon number S_0 and the frequency shift Ω. Normally, Newton Rapson (NR) method is used to obtain the solutions of the complex equation. But the equation is high nonlinear and multiple-solution. In NR method, for any longitudinal-mode solution, a pair of initial evaluated S_0 and Ω must be given, and must be close to the solution. Otherwise, the solution can not be obtained. In fact, we know it is very difficult to present all proper initial values.

In this paper, we present a Vector-Newton method which can give multiple solutions of a complex equation in the same time exactly and suitable for CAE. The small signal modulation responses of 3 phase shift (PS) DFB is investigated for the first time. Longitudinal photon density distribu-

Received 17 September 2001, revised manuscript received 28 April 2002.

tion, multiple-longitudinal-mode and AM/FM responses of 3PS-DFB and simple-DFB lasers were analyzed. The results show that modulation response characteristics of 3PS-DFB laser is as good as that of DFB, and PS can weaken the longitudinal spatial hole-burning effect and obtain a single longitudinal mode.

2 Model

The rate equations for the phase θ and photon number S can be written as[7,8]

$$\frac{d\theta(t)}{dt} = \frac{1}{2}\left\{\frac{\omega}{\bar{n}}\frac{\bar{n}}{n_g}\mathrm{Re}(\xi) + \sum_n \frac{1}{n!}\int_0^L \Gamma[\Delta N\frac{\partial}{\partial N} + \Delta S\frac{\partial}{\partial S}]^n f_A\,dz\right\} \quad (1)$$

$$\frac{dS(t)}{dt} = \left\{\frac{\omega}{\bar{n}}\frac{\bar{n}}{n_g}\mathrm{Im}(\xi) + \sum_n \frac{1}{n!}\int_0^L \Gamma[\Delta N\frac{\partial}{\partial N} + \Delta S\frac{\partial}{\partial S}]^n g_A\,dz\right\}S(t) + R_{sp} \quad (2)$$

where ω is a reference optical frequency and normally chosen to be close to the resonance frequency of the laser, $\bar{n}$ and $\bar{n}_g$ are the average refractive and group indexes, respectively. Γ is the transverse gain confinement factor. g_A and f_A are defined by

$$g_A = \frac{c}{\bar{n}_g} g_m \mathrm{Im}\left[\frac{(\alpha_m + j)\Phi^2}{\int_0^L \Phi^2 dz}\right] \quad (3)$$

$$f_A = \frac{c}{\bar{n}_g} g_m \mathrm{Re}\left[\frac{(\alpha_m + j)\Phi^2}{\int_0^L \Phi^2 dz}\right] \quad (4)$$

where $\Phi(z)$ is the normalized field distribution of the normal mode of the laser cavity, α_m is the linewidth enhancement factor, g_m is the material gain and is assumed to be

$$g_m = g_L\left[1 - \varepsilon\frac{S(t)}{\Gamma\mathcal{A}_{eff}}|\Phi(z)|^2\right] \quad (5)$$

where g_L is the linear gain, which is a function of carrier density, and ε is the material gain compression factor. For bulk material, the linear gain may be expressed by $g_L = a_N(N - N_t)$. And for quantum wells, $g_L = a_N \ln(N/N_t)$ may be used. a_N is the differential gain factor and N_t is the transparency carrier density.

The parameter ξ is the eigenvalue obtained from the solution of the following equation

$$\frac{d^2}{dz^2}\Phi(z) + \{k^2\bar{n}_{eff}^2 + k\bar{n}[\Gamma(\alpha_m + j)g_{m0} - j\Gamma\alpha_t] - k^2\xi\}\Phi(z) = 0 \quad (6)$$

where g_m is material gain coefficient, n_{eff} is effective refractive index, α_t is the material absorption coefficient and the parameter $k = \omega/c$ is the reference wave number. In Eq. (2), $\Delta N(z,t) = N(z,t) - N_0(z)$, $\Delta S(t) = S(t) - S_0$, where N_0 and S_0 are the steady-state carrier density and the photon number. The rate of spontaneous emission into the lasing mode is expressed by

$$R_{sp} = n_{sp}\int_0^L \Gamma g_B dz \Big/ \left|\int_0^L \Phi^2 dz\right|^2 \quad (7)$$

g_B is defined by

$$g_B = \frac{c}{\bar{n}_g} g_m |\Phi|^2 \quad (8)$$

The rate equation for the carrier density $N(z,t)$ is

$$\frac{dN(z,t)}{dt} = \frac{J(t)}{q} - [AN(z,t) + BN^2(z,t) + CN^3(z,t)] - \frac{S(t)}{\Gamma\mathcal{A}_{eff}} g_B \quad (9)$$

where $\mathcal{A}_{eff}$ is the effective area of the active region. $J(t)$ is the injection current density. A, B, and C are the nonradiative, bimolecular and Auger recombination coefficients. In Eq. (9), the injection current is assumed to be a constant along the cavity. Also, the carrier density is uniform over the transverse cross section of the active region and carrier diffusion, and transverse effects have been disregarded.

3 TMM and Vector-Newton methods

In this section, we will use TMM and Vector-Newton method to obtain steady-state solutions.

The coupled-mode equations can be written as[7]

$$\frac{d}{dz}R_m(z) = -j\gamma_m(z)R_m(z) - j\kappa_m L_m(z) \quad (10a)$$

$$\frac{d}{dz}L_m(z) = j\gamma_m(z)L_m(z) + j\kappa_m R_m(z) \quad (10b)$$

where

$$\gamma_m = \sqrt{\bar{n}_{eff}^2 k^2 + \bar{n}k[\bar{轴}(\alpha_m + j g_m) - j\bar{轴}(\alpha_m - \xi)^2]} - \frac{\pi}{轻} \quad (11a)$$

$$\kappa_m = (\pi/4\bar{n}_{eff}^2 轻)[2\bar{n}_{eff} n_1 + (\alpha_m + j)\bar{n} g_1/k] \quad (11b)$$

where 轻is the grating period. For a complex-coupled DFB laser, the effective refractive index n_{eff} and the lateral confinement factor 轴for the active region may be expressed by

$$n_{eff}(z) = \bar{n}_{eff} + n_1 \cos(\frac{2\pi}{轻} z) \quad (12a)$$

$$轴(z) = 轴_{avg} + 轴\cos(\frac{2\pi}{轻} z) \quad (12b)$$

where $\bar{n}_{eff}$ is the average refractive index of a reference waveguide. n_1 is the maximum effective variation. $轴_{avg}$, 轴 and g_1 are the average and the maximum variation of the gain confinement factor and gain.

The transfer matrix that maps Φfrom a location to another is given by

$$\begin{pmatrix} R_m(z) \\ L_m(z) \end{pmatrix} = \begin{pmatrix} T_{11} & T_{12} \\ T_{21} & T_{22} \end{pmatrix} \begin{pmatrix} R_m(z_0) \\ L_m(z_0) \end{pmatrix} \quad (13)$$

where

$$T_{11} = \cosh[u(z - z_0)] - j\gamma_m \sinh[u(z - z_0)]/u$$

$$T_{12} = -j\kappa_m e^{-j\Omega_g} \sinh[u(z - z_0)]/u$$

$$T_{21} = j\kappa_m e^{j\Omega_g} \sinh[u(z - z_0)]/u$$

$$T_{22} = \cosh[u(z - z_0)] + j\gamma_m \sinh[u(z - z_0)]/u$$

where $u^2 = \kappa_m^2 - \gamma_m^2$, and Ω_g is initial phase.

The boundary conditions at the laser facets are $L_m(L) = r_R R_m(L)$ and $R(0) = r_L L_m(0)$.

For the steady state, Eqs. (1), (2) and (9) reduce to

$$S_0 = -\frac{\bar{n}\bar{n}_g}{\omega} \times \frac{R_{sp}}{\mathrm{Im}(\xi)} \quad (14)$$

$$\frac{d\theta}{dt} = \frac{\omega}{\bar{n}\bar{n}_g} \mathrm{Re}(\xi) = \Omega_0 \quad (15)$$

$$\frac{J_0}{ed} - [AN_0(z) + BN_0^2(z) + CN_0^3(z)] - \frac{S_0}{●_{ff}} g_B = 0 \quad (16)$$

where unknown quantities are S_0, Ω_0, N_0 and $\Phi(z)$. At first, we construct vectors $\vec{S}_0$ and $\vec{\Omega}_0$

$$\vec{S}_0 = (S_{01}, S_{02}, \cdots S_{0i} \cdots S_{0n})$$

$$\vec{\Omega}_0 = (\Omega_{01}, \Omega_{02}, \cdots \Omega_{0j} \cdots \Omega_{0m})$$

Normally, we have $10^3 \leqslant S_{0i} \leqslant 10^6$, and $-0.1\omega \leqslant \Omega_0 \leqslant 0.1\omega$for obtaining exact results in the calculation. Certainly, vectors that have more elements and larger scope can be constructed. With the boundary condition at the left facet, initial $L(0)$ and $R(0)$ can be given. According to Eqs. (14) ~ (16), substitution of $\vec{S}_0$ and $\vec{\Omega}_0$ into (13), a matrix for final transfer results can be given as follow:

$$\begin{bmatrix} L_{1,1}(L) - r_R R_{1,1}(L) & L_{1,2}(L) - r_R R_{1,2}(L) & \cdots & L_{1,N-1}(L) - r_R R_{1,N-1}(L) & L_{1,N}(L) - r_R R_{1,N}(L) \\ L_{2,1}(L) - r_R R_{2,1}(L) & L_{2,2}(L) - r_R R_{2,2}(L) & \cdots & L_{2,N-1}(L) - r_R R_{2,N-1}(L) & L_{2,N}(L) - r_R R_{2,N}(L) \\ \cdots & \cdots & \cdots & \cdots & \cdots \\ L_{k-1,1}(L) - r_R R_{k-1,1}(L) & L_{k-1,2}(L) - r_R R_{k-1,2}(L) & \cdots & L_{k-1,N-1}(L) - r_R R_{k-1,N-1}(L) & L_{k-1,N}(L) - r_R R_{k-1,N}(L) \\ L_{k,1}(L) - r_R R_{k,1}(L) & L_{k,2}(L) - r_R R_{k,2}(L) & \cdots & L_{k,N-1}(L) - r_R R_{k,N-1}(L) & L_{k,N}(L) - r_R R_{k,N}(L) \end{bmatrix}$$

then some elements with the smallest absolute value at a local region can be obtained, i.e., some lasing modes can be obtained roughly. For obtaining accurate solutions of these regions, a Newton method is used. For a lasing mode, we assume that

$$f(S_{0,i}, \Omega_{0,j}) = L_{i,j}(L) - r_R R_{i,j}(L) \quad (17a)$$

$$f'_{S_0} = \frac{\partial f(S_{0,i} + \Omega_{0,j})}{\partial S_{0,i}} = \frac{f(S_{0,i} + \Delta S_{0,i}, \Omega_{0,j})}{\Delta S_{0,i}} \quad (17b)$$

$$f'_{\Omega_0} = \frac{\partial f(S_{0,i} + \Omega_{0,j})}{\partial \Omega_{0,j}} = \frac{f(S_{0,i}, \Omega_{0,j} + \Delta\Omega_{0,j})}{\Delta\Omega_{0,j}} \quad (17c)$$

New $S_{0,i}$ and $\Omega_{0,j}$ can be given by $S_{0,i,new} = S_{0,i} - f/f'_{S_0}$, and $\Omega_{0,j,new} = \Omega_{0,j} - f/f'_{\Omega_0}$.

Using above Vector-Newton method, all lasing mode can be obtained in the same time easily, and avoid choosing initial value and overflow problem of simple NR method.

4 Small-signal modulation responses

Suppose that $J(t)=J_0+\mathrm{Re}(\Delta J e^{j\Omega t})$, $N(z,t)=N_0(z)+\mathrm{Re}(\Delta N e^{j\Omega t})$, $S(t)=S_0+\mathrm{Re}(\Delta S e^{j\Omega t})$, $\theta(t)=\theta+\mathrm{Re}(\Delta\theta e^{j\Omega t})$, equations (1), (2) and (9) can be linearized, and utilize (14)～(16), one can obtain

$$\frac{\Delta S}{\Delta J}=\frac{c_8}{q}\int_{轴}\frac{S_0c_3+K_pn_{sp}c_4}{j\Omega+c_7}dz, \tag{18a}$$

$$\frac{\Delta\nu}{\Delta J}=\frac{1}{4\pi q}\left\{\int_{轴}\frac{c_6}{j\Omega+c_7}dz+c_8\int_{轴}\left[c_5-c_6\frac{g_B+S_0c_2}{\Phi_{ff}(j\Omega+c_7)}\right]\times dz\cdot\int_{轴}\frac{S_0c_3+K_pn_{sp}c_4}{j\Omega+c_7}dz\right\} \tag{18b}$$

where

$$c_1=-\frac{c}{n_g}\Gamma_{轴}g_L\frac{|\Phi|^2}{\Phi_{ff}}\mathrm{Im}\left[\frac{(j+\alpha_m)\Phi^2}{\int_0^L\Phi^2dz}\right]$$

$$c_2=-\frac{c}{n_g}\Gamma_{轴}g_L\frac{|\Phi|^2}{\Phi_{ff}}$$

$$c_3=\frac{c}{n_g}\frac{\partial g_L}{\partial N}\left(1-\varepsilon\frac{S_0}{\Phi_{ff}}|\Phi|^2\right)\mathrm{Im}\left[\frac{(j+\alpha_m)\Phi^2}{\int_0^L\Phi^2dz}\right]$$

$$c_4=\frac{c}{n_g}\frac{\partial g_L}{\partial N}\left(1-\varepsilon\frac{S_0}{\Phi_{ff}}|\Phi|^2\right)$$

$$c_5=-\frac{c}{n_g}\Gamma_{轴}g_L\frac{|\Phi|^2}{\Phi_{ff}}\mathrm{Re}\left[\frac{(j+\alpha_m)\Phi^2}{\int_0^L\Phi^2dz}\right]$$

$$c_6=\frac{c}{n_g}\frac{\partial g_L}{\partial N}\left(1-\varepsilon\frac{S_0}{\Phi_{ff}}|\Phi|^2\right)\mathrm{Re}\left[\frac{(j+\alpha_m)\Phi^2}{\int_0^L\Phi^2dz}\right]$$

$$c_7=A+2BN_0+3CN_0^2+\frac{c_4S_0}{\Phi_{ff}}$$

$$c_8=\left[j\Omega+c_9+\int_{轴}(S_0c_3+K_pn_{sp}c_4)\times\frac{g_B+S_0c_2}{\Phi_{ff}(j\Omega+c_7)}dz\right]^{-1}$$

$$c_9=\frac{R_{sp}}{S_0}-\int_{轴}(c_1S_0+c_2K_pn_{sp})\,dz$$

where $\Delta S/\Delta J$ is the amplitude modulation (AM) response and $\Delta\nu/\Delta J=j\Omega\Delta\theta/(2\pi\Delta J)$ is the frequency modulation (FM) response.

5 Results of analysis

Using above models and Vector-Newton method, the characteristics of steady multiple-longitudinal-mode and AM/FM modulation responses of a ^{3}PS-DFB are analyzed. Parameters used in the simulation are presented in Table 1. Locations of phase shift lie in $L/4$, $L/2$ and $3L/4$, and all values of phase shift are $\pi/3$. In our calculation, 65, 75, 90 and 110 mA four injection currents are analyzed. A simple DFB laser without phase shift is analyzed in the same time. Two vectors are constructed, and each one included 50 elements. For solving equations for Φ, the whole structure is subdivided by several sections along the cavity. Thirty sections are enough for normal analysis.

Talbe 1 Material and geometrical parameters of the simulated PS-DFB laser

Shockley-Read-Hall recombination coefficient	$A=4\times10^8\,s^{-1}$
Bimolecular recombination coefficient	$B=1\times10^{-10}\,cm^{-3}\cdot s^{-1}$
Auger recombination coefficient	$C=2\times10^{-29}\,cm^{-6}\cdot s^{-1}$
Linewidth enhancement factor	$\alpha_m=-3$
Absorption loss	轴 $\alpha_i=25\,cm^{-1}$
Differential gain parameter	$\alpha_1=3\times10^{-16}\,cm^3$
Gain saturation factor	$\varepsilon=1.5\times10^{-17}\,cm^3$
Transparency carrier concentration	$N_t=1.5\times10^{18}\,cm^{-3}$
Facet reflectivity	$r_R=r_L=0$
Cavity length	$L=5\times10^{-2}\,cm$
Average group refraction index	$\bar{n}_g=3.5294$
Average refraction index	$\bar{n}=3.256$
Average effective refraction index	$\bar{n}_{eff}=3.3136$
Average confinement factor	轴 $=0.3$
Grating period	栅 $=0.235\,\mu m$
Coupling coefficient	$\kappa=40\,cm^{-1}$
Thickness of the active region	$d=0.12\,\mu m$

It is observed that LHSB occurs at both ^{3}PS-DFB and simple DFB lasers, as shown in Fig. 1. Phase shifts affect photon distribution in the cavity, which weaken LHSB effect as a whole. We also observe that LHSB is evident at high bias. Figure 2

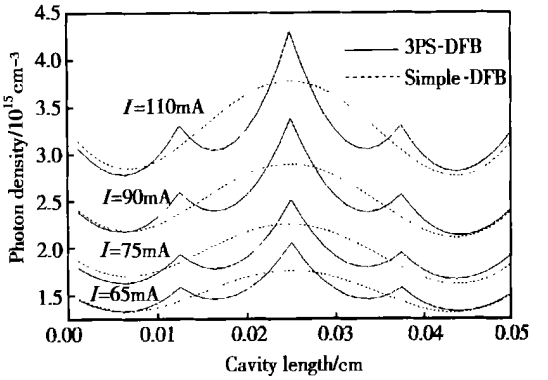

Fig. 1 Longitudinal distribution of the photon density inside ^{3}PS-DFB and simple-DFB LDs

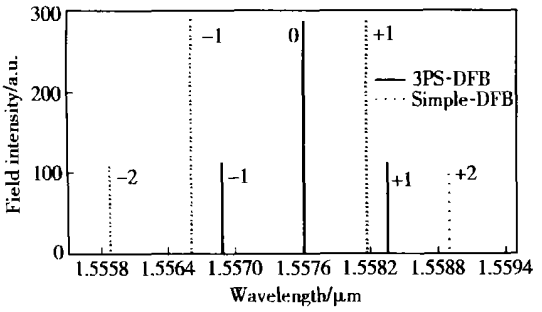

Fig. 2　Multiple-longitudinal-mode distribution of 3PS-DFB and simple-DFB LDs

describes multiple-longitudinal-mode distribution of 3PS-DFB and simple-DFB laser at 110mA injection current. It can be observed that phase shifts change the position of longitudinal modes and two main modes of simple DFB laser turn into one main mode of 3PS-DFB, which present a method to obtain single longitudinal mode. AM modulation response of small signal is given in Fig. 3, and FM modulation response in Fig. 4. At high injection current, intensity of responses decreases, while response frequency increases. Phase shifts affect AM

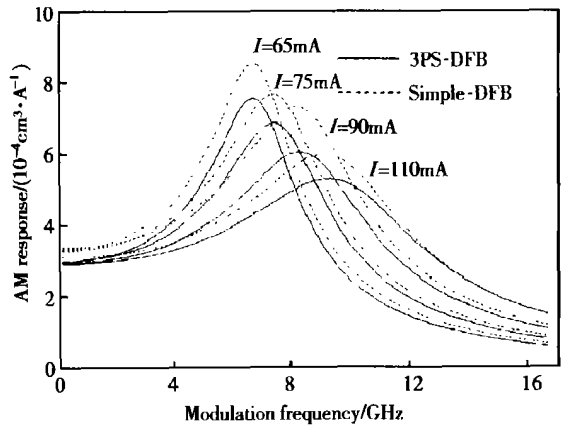

Fig. 3　AM responses of 3PS-DFB and simple-DFB LDs with different injection currents

response evidently. For FM modulation response, phase shifts have an effect on intensity of response, but not change response frequency. These results agreeed with Ref. [8] for a normal DFB laser. In the calculation, we find Vector-Newton method can give all longitudinal modes solutions exactly and avoid choosing initial value and overflow problem by using simple NR method.

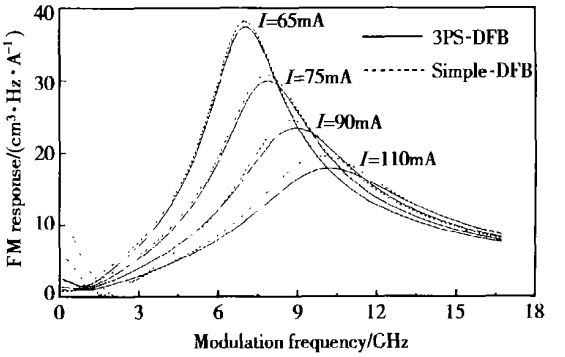

Fig. 4　Fm responses of 3PS-DFB and simple-DFB LDs with different injection currents

6 Conclusion

A numerical model for steady state simulation and analytical expressions for the AM and FM modulation responses of PS-DFB lasers are presented. Vector-Newton method is applied to obtain multiple-longitudinal-mode of lasers. Further, this method can be used in 2-D and 3-D simulation, which make multiple-solution of high nonlinear equation obtained easily. AM and FM modulation responses of 3PS-DFB and simple DFB lasers are analyzed. The results show that PS can weaken LHSB effect and are in favor of single longitudinal mode operating.

References

[1] Vankwikelberge P, Morthier G, Baets R. CLADISS-A longitudinal multi-mode model for the analysis of the static, dynamic and static behavior of diode lasers with DFB. IEEE J Quantum Electron, 1990, 26(2): 1728

[2] Tromborg B, Olesen H, Pan X. Theory of linewidth for multi-electrode laser diodes with spatially distributed noise sources. IEEE J Quantum Electron, 1991, 27(2): 178

[3] Zhang L M, Carrol J. Large-signal dynamic model of DFB lasers. IEEE J Quantum Electron, 1992, 28(3): 604

[4] Sarangan A M, Huang W P, Li G P, et al. A ridge waveguide DFB laser model including transverse carrier and optical effects. IEEE J Quantum Electron, 1996, 32(3): 408

[5] Yu S F. A quasithree-dimensional large-signal dynamic model of distributed feedback lasers. IEEE J Quantum Electron, 1996, 32(3): 408

[6] Wunsche H J, Bandelow U, Wenzel H. Calculation of combined lateral and longitudinal spatial hole burning in $\lambda/4$ shifted DFB lasers. IEEE J Quantum Electron, 1993, 29(6): 1751

[7] Li Xun, Sadovnikov A D, Huang W P, et al. A physics-based three-dimensional model for distributed feedback laser diode. IEEE J Quantum Electron, 1998, 34(9): 1545

[8] Sadovnikov A D, Li Xun, Huang W P. A two-dimensional DFB laser model accounting for carrier transport effects. IEEE J Quantum Electron, 1995, 31(10): 1856

半导体相移分布反馈激光器模式及调制相应特性的研究——牛顿-矢量方法的应用

张冶金[1] 朱 林[1] 高志国[1] 陈明华[1] 董 毅[1] 陈维友[2] 刘式墉[2] 谢世钟[1]

([1] 清华大学电子工程系，北京 100084)

([2] 吉林大学电子工程系，长春 130023)

摘要：给出了适于分析 DFB 激光器稳态特性的数值模型和分析振幅及频率调制响应特性的解析模型. 研究了 3 相移 DFB 激光器的调制响应特性，并提出了一种能够快速精确得到 DFB 激光器多个模式解的新方法——矢量牛顿法. 该方法将稳定的矢量法与精确的牛顿法结合，保证了求解质量. 实践表明该方法非常适合于求解高度非线性方程的多解问题. 用此方法，研究了 3 相移及简单 DFB 激光器的纵向光子浓度分布，纵模及调制响应特性. 结果表明，3 相移 DFB 具有与简单的 DFB 激光器同样好的调制响应特性，相移的引入在一定程度上抑制了纵向空间烧孔效应，并且有利于 DFB 激光器的单模输出.

关键词：相移；DFB；矢量；单模；纵向空间烧孔效应；调制响应

PACC：4255P；4260；7340L；7280

中图分类号：TN248.4 **文献标识码**：A **文章编号**：0253-4177(2002)09-0935-06

2001-09-17 收到，2002-04-28 定稿